Research Article | Vol. 25, No. 12 | 12 Jun 2017 | OPTICS EXPRESS 13372
Optics EXPRESS

Frequency gating to isolate single attosecond pulses with overdense plasmas using particle-in-cell simulations

M. BLANCO* AND M.T. FLORES-ARIAS

Photonics4Life Group, Departamento de Física Aplicada, Facultad de Física, Campus Vida, Universidade de Santiago de Compostela, 15782 Santiago de Compostela, Spain
*manuel.blanco.fraga@usc.es

Abstract: We present the isolation of single attosecond pulses for multi-cycle and few-cycle laser pulses from high harmonic generation in overdense plasmas, calculated with particle-in-cell simulations. By the combination of two laser pulses of equal amplitude and a small frequency shift between them, we demonstrate that it is possible to shorten the region in which the laser pulse is most intense, therefore restricting the generation of high harmonic orders in the form of attosecond pulses to a narrower time window. The creation of this window is achieved due to the combination of the laser pulse envelope and the slow oscillating wave obtained from the coherent sum of the two pulses. A parametric scan, performed with particle-in-cell simulations, reveals how the pulse isolation behaves for different input laser pulse lengths and which are the optimal frequency shifts between the two laser pulses in each case, giving the conditions for having a good isolation of an attosecond pulse when working with laser-plasma interaction in overdense targets.

OCIS codes: (190.0190) Nonlinear optics; (190.7110) Ultrafast nonlinear optics; (350.5400) Plasmas.

References and links

1. P. Antoine, A. L'Huillier, and M. Lewenstein, "Attosecond pulse trains using high order harmonics," Phys. Rev. Lett. **77**(7), 1234-1237 (1996).
2. I. Christov, M. Murnane, and H. Kapteyn, "High-harmonic generation of attosecond pulses in the "single-cycle" regime," Phys. Rev. Lett. **78**(7), 1251-1254 (1997).
3. J. Mauritsson, P. Johnsson, E. Gustafsson, A. L'Huillier, K. J. Schafer, and M. B. Gaarde, "Attosecond pulse trains generated using two color laser fields," Phys. Rev. Lett. **97**, 013001 (2006).
4. L. Plaja, L. Roso, K. Rzazewski, and M. Lewenstein, "Generation of attosecond pulse trains during the reflection of a very intense laser on a solid surface," J. Opt. Soc. Am. B **15**(7), 1904-1911 (1998).
5. A. S. Pirozhkov, S. V. Bulanov, T. Z. Esirkepov, M. Mori, A. Sagisaka, and H. Daido, "Attosecond pulse generation in the relativistic regime of the laser-foil interaction: The sliding mirror model," Phys. Plasmas **13**, 013107 (2006).
6. S. G. Rykovanov, M. Geissler, J. Meyer-ter Vehn, and G. D. Tsakiris, "Intense single attosecond pulses from surface harmonics using the polarization gating technique," New J. Phys. **10**, 025025 (2008).
7. U. Teubner, and P. Gibbon, "High-order harmonics from laser-irradiated plasma surfaces," Rev. Mod. Phys. **81**, 445-479 (2009).
8. C. Thaury, and F. Quéré, "High-order harmonic and attosecond pulse generation on plasma mirrors: basic mechanisms," J. Phys. B **43**, 213001 (2010).
9. G. Ma, W. Dallari, A. Borot, F. Krausz, W. Yu, G. D. Tsakiris, and L. Veisz, "Intense isolated attosecond pulse generation from relativistic laser plasmas using few-cycle laser pulses," Phys. Plasmas **22**, 033105 (2015).
10. P. M. Paul, E. S. Toma, P. Breger, G. Mullot, F. AugÃl', P. Balcou, H. G. Muller, and P. Agostini, "Observation of a train of attosecond pulses from high harmonic generation," Science **292**, 1689–1692 (2001).
11. G. Sansone, L. Poletto, and M. Nisoli, "High-energy attosecond light sources," Nat. Photon. **5**, 655–663 (2011).
12. A. L. Cavalieri, N. Müller, T. Uphues, V. S. Yakovlev, A. Baltuska, B. Horvath, B. Schmidt, L. Blümel, R. Holzwarth, S. Hendel, M. Drescher, U. Kleineberg, P. M. Echenique, R. Kienberger, F. Krausz, and U. Heinzmann, "Attosecond spectroscopy in condensed matter," Nature **449**, 1029–1032 (2007).
13. M. Schultze, M. Ulberacker, T. Uphues, A. J. Verhoef, V. Yakovlev, M. F. Kling, J. Rausehenberger, N. M. Kabachnik, H. Schröder, M. Lezius, K. L. Kompa, H. G. Muller, M. J. J. Vrakkinig, S. Hendel, U. Kleineberg, U. Heinzmann, M. Drescher, and F. Krausz, "Attosecond real-time observation of electron tunnelling in atoms," Nature **446**, 627–632 (2007).
14. W. Theobald, R. Häßner, C. Wülker, and R. Sauerbrey, "Temporally Resolved Measurement of Electron Densities $> 10^{23}$ cm^{-3} with High Harmonics," Phys. Rev. Lett. **77**(2), 298-301 (1996).

#293263 https://doi.org/10.1364/OE.25.013372
Journal © 2017 Received 20 Apr 2017; revised 27 May 2017; accepted 29 May 2017; published 2 Jun 2017

Optics EXPRESS

15. D. Descamps, C. Lyngå, J. Norin, A. L'huillier, C. G. Wahlström, J. F. Hergott, H. Merdji, P. Salières, M. Bellini, and T. W. Hänsch, "Extreme ultraviolet interferometry measurements with high-order harmonics," Opt. Lett. **25**(2), 135–137 (2000).
16. L. Nugent-Glandorf, M. Scheer, D. A. Samuels, A. M. Mulhisen, E. R. Grant, X. Yang, V. M. Bierbaum, and S. R. Leone, "Ultrafast Time-Resolved Soft X-Ray Photoelectron Spectroscopy of Dissociating Br_2," Phys. Rev. Lety. **87**(19), 193002 (2001).
17. A. Malvache, A. Borot, F. Quéré, and R. Lopez-Martens, "Coherent wake emission spectroscopy as a probe of steep plasma density profiles," Phys. Rev. E **87**, 035101 (2013).
18. A. Debayle, J. Sanz, and L. Gremillet, "Self-consistent theory of high-order harmonic generation by relativistic plasma mirror," Phys. Rev. E **92**, 053108 (2015).
19. A. Debayle, J. Sanz, L. Gremillet, and K. Mima, "Toward a self-consistent model of the interaction between an ultra-intense, normally incident laser pulse with an overdense plasma," Phys. Plasmas **20**, 053107 (2013).
20. J. Sanz, A. Debayle, and K. Mima, "Model for ultraintense laser-plasma interaction at normal incidence," Phys. Rev. E **85**, 046411 (2012).
21. B. Bezzerides, R. D. Jones, and D. W. Forslund, "Plasma Mechanism for Ultraviolet Harmonic Radiation Due to Intense CO_2 Light," Phys. Rev. Lett. **49**(3), 202-205 (1982).
22. R. Lichters, J. Meyer-ter-Vehn, and A. Pukhov, "Short-pulse laser harmonics from oscillating plasma surfaces driven at relativistic intensity," Phys. Plasmas **3**(9), 3425-3437 (1996).
23. A. A. Gonoskov, A. V. Korzhimanov, A. V. Kim, M. Marklund, and A. M. Sergeev, "Ultrarelativistic nanoplasmonics as a route towards extreme-intensity attosecond pulses," Phys. Rev. E **84**, 046403 (2011).
24. H. Vincenti, S. Monchocé, S. Kahaly, G. Bonnaud, P. Martin, and F. Quéré, "Optical properties of relativistic plasma mirrors," Nat. Commun. **5**, 3403 (2014).
25. P. Agostini, and L. F. DiMauro, "The physics of attosecond light pulses," Rep. Prog. Phys. **67**, 813-855 (2004).
26. P. B. Corkum, and F. Krausz, "Attosecond science," Nat. Phys. **3**, 381-387 (2007)
27. A. P. Tarasevitch, R. Kohn, and D. von der Linde, "Towards intense attosecond pulses: using two beams for high order harmonic generation from solid targets," J. Phys. B **42**, 134006 (2009).
28. A. Tarasevitch, and D. von der Linde, "High order harmonic generation from solid targets: Towards intense attosecond pulses," Eur. Phys. J. Spec. Top. **175**, 35-41 (2009).
29. M. R. Edwards, and J. M. Mikhailova, "Waveform-Controlled Relativistic High-Order-Harmonic Generation," Phys. Rev. Lett. **117**, 125001 (2016).
30. G. D. Tsakiris, K. Eidmann, J. Meyer-ter Vehn, and F. Krausz, "Route to intense single attosecond pulses," New J. Phys. **8**(1), 19 (2006).
31. P. B. Corkum, N. H. Burnett, and M. Y. Ivanov, "Subfemtosecond pulses," Opt. Lett. **19**, 1870-1872 (1994).
32. G. Sansone, E. Benedetti, F. Calegari, C. Vozzi, L. Avaldi, R. Flammini, L. Poletto, P. Villoresi, C. Altucci, R. Velotta, S. Stagira, S. De Silvestri, and M. Nisoli, "Isolated Single-Cycle Attosecond Pulses," Science **314**, 443-446 (2006).
33. F. Cambronero-López, M. Blanco, C. Ruiz, M. T. Flores-Arias, and C. Bao-Varela, "Polarization gating using cross-polarized wave generation with multicycle lasers to produce isolated attosecond pulses in overdense media," J. Opt. Soc. Am. B **34**(4), 843-849 (2017).
34. E. Balogh, C. Zhang, T. Ruchon, J.-F. Hergott, F. Quere, P. Corkum, C. H. Nam, and K. T. Kim, "Dynamic wavefront rotation in the attosecond lighthouse," Optica **4**(1), 48-53 (2017).
35. J. A. Wheeler, A. Borot, S. Monchocé, H. Vincenti, A. Ricci, A. Malvache, R. Lopez-Martens, and F. Quéré, "Attosecond lighthouses from plasma mirrors," Nat. Photonics **6**, 829-833 (2012).
36. H. Vincenti, and F. Quéré, "Attosecond lighthouses: how to use spatiotemporally coupled light fields to generate isolated attosecond pulses," Phys. Rev. Lett. **108**, 113904 (2012).
37. I. J. Sola, E. Mével, L. Elouga, E. Constant, V. Strelkov, L. Poletto, P. Villoresi, E. Benedetti, J.-P. Caumes, S. Stagira, C. Vozzi, G. Sansone, and M. Nisoli, "Controlling attosecond electron dynamics by phase-stabilized polarization gating," Nat. Phys. **2**, 319-322 (2006).
38. J. J. Carrera, X. M. Tong, and S. I. Chu, "Creation and control of a single coherent attosecond xuv pulse by few-cycle intense laser pulses," Phys. Rev. A **74**, 023404 (2006).
39. G. Sansone, E. Benedetti, J. P. Caumes, S. Stagira, C. Vozzi, M. Nisoli, L. Poletto, P. Villoresi, V. Strelkov, I. Sola, L. B. Elouga, A. Zaïr, E. Mèvel, and E. Constant, "Shaping of attosecond pulses by phase-stabilized polarization gating," Phys. Rev. A **80**, 063837 (2009).
40. T. Pfeifer, L. Gallmann, M. J. Abel, P. M. Nagel, D. M. Neumark, and S. R. Leone, "Heterodyne Mixing of Laser Fields for Temporal Gating of High-Order Harmonic Generation," Phys. Rev. Lett. **97**, 163901 (2006).
41. H. Merdji, T. Auguste, W. Boutu, J. P. Caumes, B. Carré, T. Pfeifer, A. Jullien, D. M. Neumark, and S. R. Leone, "Isolated attosecond pulses using a detuned second-harmonic field," Opt. Lett. **32**(21), 3134-3136 (2007).
42. E. J. Takahashi, P. Lan, O. D. Mücke, Y. Nabekawa, and J. Midorikawa, "Infrared Two-Color Multicycle Laser Field Synthesis for Generating an Intense Attosecond Pulse," Phys. Rev. Lett. **104**, 233901 (2010).
43. E. J. Takahashi, P. Lan, O. D. Mücke, Y. Nabekawa, and J. Midorikawa, "Attosecond nonlinear optics using gigawatt-scale isolated attosecond pulses," Nat. Commun. **4**, 2691 (2013).
44. S. Haessler, T. Balčiūnas, G. Fan, L. E. Chipperfield, and A. Baltuška, "Enhanced multi-colour gating for the generation of high-power isolated attosecond pulses," Sci. Rep. **5**, 10084 (2015).

Optics EXPRESS

45. M. R. Edwards, V. T. Platonenko, and J. M. Mikhailova, "Enhanced attosecond bursts of relativistic high-order harmonics driven by two-color fields," Opt. Lett. **39**(24), 6823-6826 (2014).
46. S. Mirzanejad, and M. Salehi, "Two-color high-order-harmonic generation: Relativistic mirror effects and attosecond pulses," Phys. Rev. A **87**, 063815 (2013).
47. R. A. Fonseca, L. O. Silva, F. S. Tsung, V. K. Decyk, W. Lu, C. Ren, W. B. Mori, S. Deng, S. Lee, T. Katsouleas, and J. C. Adam, "OSIRIS: A Three-Dimensional, Fully Relativistic Particle in Cell Code for Modeling Plasma Based Accelerators," in *Lecture Notes in Computer Science, vol 2331,* P. M. A. Sloot, A. G. Hoekstra, C. J. K. Tan, J. J. Dongarra, eds. (Springer, 2002), pp. 342–351.
48. R. A. Fonseca, J. Vieira, F. Fiuza, A. Davidson, F. S. Tsung, W. B. Mori, and L. O. Silva, "Exploiting multi-scale parallelism for large scale numerical modelling of laser wakefield accelerators," Plasma Phys. Control. Fusion **55**, 124011 (2013).
49. R. A. Fonseca, S. F. Martins, L. O. Silva, J. W. Tonge, F. S. Tsung, and W. B. Mori, "One-to-one direct modeling of experiments and astrophysical scenarios: pushing the envelope on kinetic plasma simulations," Plasma Phys. Control. Fusion **50**, 124034 (2008).
50. A. Bourdier, "Oblique incidence of a strong electromagnetic wave on a cold inhomogeneous electron plasma. Relativistic effects," Phys. Fluids **26**, 1804–1807 (1983).

1. Introduction

Attoscience is a very interesting field that has gained attention over the past decades. One of its main areas of research is the generation of controllable ultrashort radiation sources [1–11] to be used in different applications [11–17] or to study the nature of their generation [7, 8, 18–26]. These ultrashort sources are usually created through the interaction between an intense laser pulse with a gas [1–3, 11] or a solid [4–8, 11, 20–24, 27–29] medium, such that because of this interaction integer multiples of the central laser wavelength are generated. This high harmonic generation (HHG) occurs periodically during the laser field oscillations, being concentrated in trains of ultrashort pulses. Via this mechanism it has been possible to obtain radiation sources with widths in the tens and hundreds of attoseconds with a spectral content that extends beyond the XUV [25–28, 30].

The generation of these pulses in gas or solid media relies on different mechanisms and occurs for different regimes of laser intensity. In gas media HHG is generated due to a nonlinear quantum process, in which the laser pulse interacts with the atoms and molecules in the medium and the harmonic spectrum is carried in the transmitted field [1–3, 11]. In solid media, typically the pre-pulse or the front part of the laser pulse ionizes the solid surface, creating a plasma with a high density that reflects the laser pulse. The rapid oscillations of the electrons over the ion background, caused by the laser field, generate periodic bursts of radiation that appear as attosecond pulses in the reflected field [4–8, 11, 20–24, 27–29]. In the case of solid targets, the generation of these pulses is a relativistic effect [7, 8, 18–24]. Although gas harmonics have been studied for a longer time and there is a greater knowledge about the process and how to control it, there are several limitations that can be overcomed by using solid targets, namely the possibility of using higher laser intensities and having higher harmonic cutoffs, being therefore able to obtain more intense and more energetic ultrashort pulses using solid targets.

Attosecond pulses and their harmonic spectrum are generated periodically during the pulse oscillations as trains of pulses. Some applications require the use of a single pulse [12–14], therefore techniques to isolate a single ultrashort pulse have been developed over the years. In solid media, the isolation techniques rely on several methods, namely: the intensity gating method [30], based on the fact that the most intense ultrashort pulses are associated with the most intense oscillations of the laser pulse; the polarization gating method [6, 31–33], consisting on the use of laser pulses with a time-dependent polarization state; the attosecond lighthouse [34–36] that uses pulses with a tilted wavefront to generate each attosecond pulse of the train in a different direction and therefore isolate them. In gas media there are similar mechanisms to obtain also isolated attosecond pulses [37–39].

In this paper we propose a new method to obtain isolated attosecond pulses from laser-plasma

Optics EXPRESS

interaction in overdense plasmas. It basically consists on the coherent combination of two laser pulses with equal amplitude and a non-integer ratio between their central frequencies, such that a beating pattern is formed in the resulting field. This is a well-known effect in frequency synthesis. The coherent sum of the two pulses generates a slow oscillating component that, combined with the pulse envelope, restricts the most intense region of the new pulse to a narrower window than this at the original pulse, being able to reduce the number of pulses in the train, even isolating one single pulse. Setups involving the coherent combination of more than one pulse and forming a beating pattern have been already studied extensively as a mean to isolate single attosecond pulses in HHG using gas targets [40–44], where it is possible to achieve isolated attosecond pulses very efficiently, even for multicycle laser pulses. In the case of laser-plasma interaction using solid targets, the effect of the combination of multiple laser pulses has been also studied, but to our knowledge never with the purpose and approach taken in this paper [27–29, 45, 46].

2. Results

Let us consider two short pulses with frequencies ω_1 and ω_2, respectively, given by $E_j = \Gamma(t)\cos(\omega_j t)$, where $\Gamma(t)$ is the envelope function. The coherent sum of these two waves can be written as:

$$E = E_1 + E_2 = 2\Gamma(t)\cos\left(\frac{\omega_2+\omega_1}{2}t\right)\cos\left(\frac{\omega_2-\omega_1}{2}t\right) \quad (1)$$

This means that there is a fast and slow oscillating wave. The frequency of the slow oscillating wave $(\omega_2 - \omega_1)$ can be tuned, in combination with the pulse envelope $\Gamma(t)$, by varying the frequency values, to create a beating pattern that yields to a narrower intense region. Figure 1 depicts several cases with different frequency shifts, using a gaussian envelope function given by $\Gamma(t) = e^{-4log(2)(t/\tau)^2}$. We have used as principal wavelength of $\lambda_1 = 800$ nm ($\omega_1 = 2\pi\frac{c}{\lambda_1}$) and a Full Width Half Maximum (FWHM) of $\tau = 20$ fs.

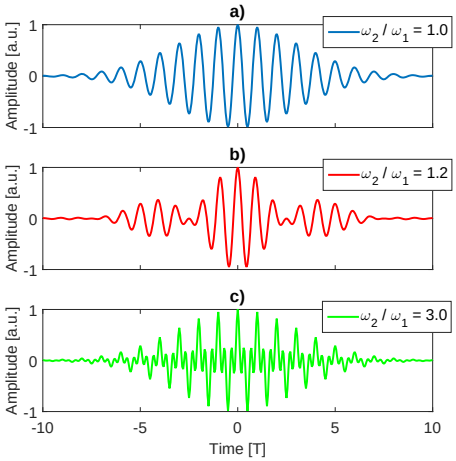

Fig. 1. Laser pulses obtained through the combination of two frequency shifted pulses of (a) equal frequency, (b) a ratio of $\omega_2/\omega_1 = 1.2$ and (c) a ratio $\omega_2/\omega_1 = 3$. The reference wavelength is $\lambda_1 = 800$ nm and the FWHM is $\tau = 20$ fs. The x axis is in units of the laser period, T.

It can be seen in Fig. 1(b) how the central and most intense part of the pulse becomes narrower when the frequency shift between the two pulses is tuned properly. Therefore HHG will be

Optics EXPRESS

favoured for this smaller window of time. If the frequency shift is higher, such as in Fig. 1(c), fast oscillating corrections will be added to the original shape of the pulse, but the envelope of the most intense peaks will remain unchanged, disappearing the small temporal window from Fig. 1(b).

To check for the validity of this mechanism, we perform Particle-In-Cell (PIC) simulations with the OSIRIS code [47–49]. The simulations are done in 1D using p-polarized pulses with the boosted frame method [6,23,50], to simulate the angle of incidence of the beam without the need of 2D simulations, more demanding computationally. The target is composed of electrons and heavy ions with a number density of $100n_c$, where n_c is the critical density of the plasma. We assume a steep density profile. The number of particles per cell is 200. The temporal and spatial resolution of the simulation box are $0.0025/\omega$ and $0.005c/\omega$, respectively, where ω is the frequency of the laser pulse, with a wavelength of $\lambda = 800$ nm. The laser pulses are initialized inside the simulation box with a gaussian profile, a dimensionless amplitude of $a_0 = 4$ and an angle of incidence of 45^o. The simulation runs until the whole pulse is reflected, that is the time that it would take it to return to its original position if the target would be a perfect mirror. The train of attosecond pulses is obtained by performing the inverse Fourier transform to the harmonic orders between the $5^{'h}$ and the $50^{'h}$ in the reflected field.

In order to study this mechanism and achieve an optimal configuration to produce the isolation of one single pulse or a few ultrashort attosecond pulses, we have evaluated different ratios between the central frequency of both laser pulses. Figure 2 displays the result obtained by properly tuning the frequency shift to a ratio of $\omega_2/\omega_1 = 1.3$. In this case, in which a laser pulse with a FWHM of $\tau = 25$ fs has been used, it leads to almost the isolation of a single attosecond pulse in the filtered train of pulses. It can be seen clearly in the oscillations of the electron density that the most intense oscillations, associated to the generation of the most intense pulses with a higher frequency content, are confined into a shorter temporal window.

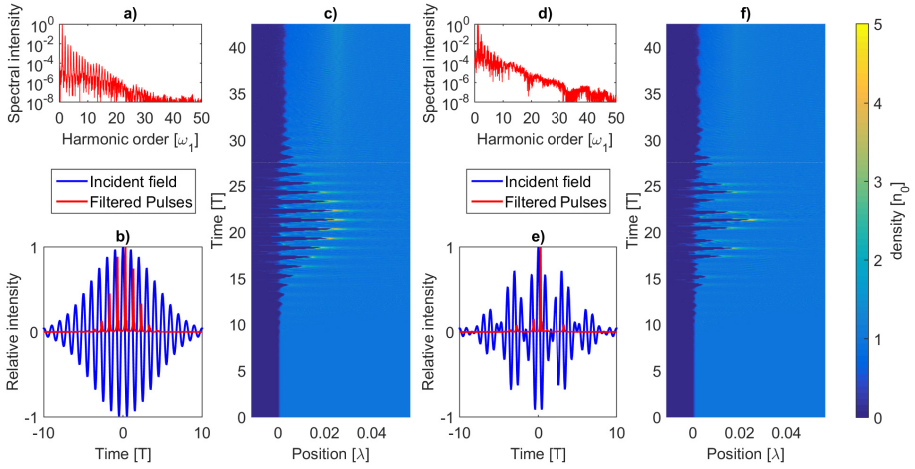

Fig. 2. Comparison of two simulations to depict the isolation of a single attosecond pulse in the filtered pulse train. Both simulations are performed with two pulses of (a)-(c) equal frequency and (d)-(f) a frequency ratio of $\omega_2/\omega_1 = 1.3$. The comparison between the reflected pulse trains in (b) and (e) and the electron density oscillations in (c) and (f) clearly shows the narrowing of the HHG window.

Figure 2 proves that this method is able to shorten the pulse train substantially. Hence we proceed to perform a proper parametric scan in order to unravel if there is an optimal frequency ratio for pulse isolation, and the relation between the FWHM of the input pulse and the isolation

Optics EXPRESS

efficiency. We assume as criteria to evaluate the goodness of our results the number of pulses contained in the reflected train, as well as their intensity in relation to the most intense one. Let us define the isolation efficiency (ξ) as:

$$\xi = \prod_{j=1}^{N-1} \left(1 - \frac{I_j}{I_0}\right) \tag{2}$$

where $N > 1$ represents the number of pulses in the train with a peak intensity I_j above 5% of the maximum peak. If $\xi = 1$ the isolation is perfect. Increasing the number of pulses in the train or their relative intensity to the most intense pulse, provokes a decrease in ξ up to the limit when the pulse cannot be regarded as isolated anymore ($\xi \sim 0$). This definition of the efficiency permits us to obtain a low isolation efficiency both if there are few pulses in the train with a high intensity in relation to the most intense pulse or if there are several pulses in the train with a low relative intensity.

We have performed simulations for frequency ratios (ω_2/ω_1) between the values 1 and 2 and for several FWHMs in between 5 fs and 55 fs. For each pulse width we have checked for the frequency ratio that yields to the highest isolation efficiency and the corresponding efficiency. Figure 3 shows the results obtained for input pulses with a FWHM of (a) 10 fs, (b) 25 fs and (c) 40 fs. In the left column it is shown 2D maps that depict, for each frequency ratio, the pulse train obtained over time (normalized to the maximum at each frequency ratio, for the sake of visualization), these 2D maps demonstrate that the shape of the pulse train over time varies for different frequency ratios. In the two columns on the right, the isolation efficiency and the intensity of the most intense pulse in the train are shown, respectively, the former is plotted to demonstrate quantitatively that the isolation efficiency varies with the frequency ratio and the latter to show the normalization factor (the maximum intensity on the pulse train) for each frequency ratio in the normalized 2D maps of the left column.

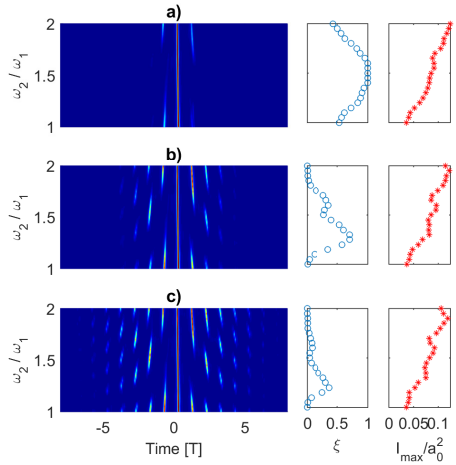

Fig. 3. Results of the parametric scan for different pulse widths of (a) 10 fs, (b) 25 fs and (c) 40 fs. In the left column it is displayed the train of pulses over time for each frequency ratio. The signal is normalized to the most intense pulse in each frequency ratio. In the right columns the isolation efficiency (ξ) and the maximum intensity in the central pulse of the train is depicted for each frequency ratio.

Figure 3 reveals several interesting features of this gating method. First of all, it is clear that different isolation efficiencies can be obtained by tuning the frequency shift between the two

Optics EXPRESS

pulses. The optimal ratio for isolation is shifted upwards as the pulse FWHM decreases. This makes sense, because for a narrower envelope the "slow" frequency ($\omega_2 - \omega_1$) must be increased in order to oscillate within the envelope width. Secondly, as the ratio between frequencies goes beyond this optimal value, the oscillatory laser field peaks return to their original position with high frequency corrections (as shown in Fig. 1(c)), causing the generation or more complex dynamics at the plasma surface and the creation of pulse trains with several ultrashort pulses in them, with a higher peak intensity, as it can be observed in Fig. 3 when the frequency ratio approaches the value 2. It can be also noted that, as the FWHM of the pulse increases, the maximum isolation efficiency decreases, therefore establishing a limitation for this gating method. On the other hand, if the pulse width is too low, the pulse envelope itself isolates a single attosecond pulse, due to the existence of a few oscillations within the pulse width. In this case the use of a gating method becomes pointless and high isolation efficiencies are achieved for several frequency shifts. An example is shown in Fig. 3(a), where for a frequency ratio equal to the unity (i.e. the pulse original shape), for a pulse with a FWHM of 10 fs, the isolation efficiency is nearly the same as in the most optimal case for a pulse with a FWHM of 40 fs, as shown in Fig. 3(c). It is clear that there is a frequency ratio for which the isolation is optimal, and that it varies with the pulse width.

To further emphasize these results, we have also analyzed how the train of attosecond pulses is changed by fixing a certain frequency ratio and varying the laser pulse FWHM. Figure 4 shows the incident laser field as well as the reflected train of pulses for two fixed frequency ratios and two different values of the FWHM. It is clear from this Fig. that the optimal frequency ratio varies for different pulse widths. In Fig. 4(a), in which a frequency ratio of 1.4 has been used, it can be seen that the isolation is better for the width of 15 fs, in comparison with the case in Fig. 4(b), in which a frequency ratio of 1.2 has been used, whereas the opposite occurs for the pulse with a FWHM of 30 fs, in Figs. 4(c) and 4(d), where the isolation efficiency is higher for a ratio of 1.2.

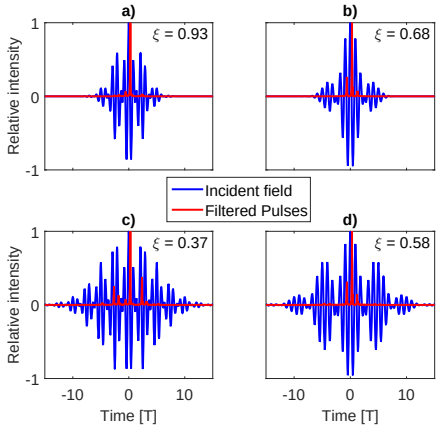

Fig. 4. Trains of pulses generated for the mix of pulses with a frequency ratio of (a)-(c) $\omega_2/\omega_1 = 1.4$ and (b)-(d) $\omega_2/\omega_1 = 1.2$. The pulses FWHM are (a)-(b) 15 fs and (c)-(d) 30 fs. The isolation efficiency is shown in the upper-right corner of each plot.

The 2D maps in the left column of Fig. 3 show an asymmetry in the pulse train in relation to the location of the central pulse, this is more obvious in Figs. 3(b) and 3(c), where the train of pulses is longer than in Fig. 3(a), and the central attosecond pulse does not get fully isolated, even in the most optimal configuration. A variation of the carrier envelope phase (CEP) of the input laser pulse could vary the shape of the train, contributing to an enhancement or a

Optics EXPRESS

deterioration of the isolation efficiency. We have analyzed the effect of varying the CEP of the input pulse from 0^o to 360^o for the most optimal ratio for two pulses with a FWHM of 25 fs ($\omega_2/\omega_1 = 1.3$). Figure 5(a) shows a 2D map of the resulting pulse train for each CEP, normalized to the maximum intensity at each CEP for the sake of visualization. A change in the global phase of the input pulse affects the shape of the attosecond pulse train, as it is shown in Fig. 5(b). In this figure we can observe the isolation efficiency for each CEP, revealing how crucial is to choose the CEP wisely. Increasing the CEP shows a decrease in the isolation efficiency until a minimum is reached at a CEP of 130^o, where it becomes almost zero. After this value, the isolation efficiency increases again until achieving an approximately constant value in the CEP range $[260^o,\ 360^o]$. The plots in Figs. 5(c) and 5(d) display the input laser pulse and the obtained attosecond pulse train for the optimal isolation case with a CEP of 0^o and for the less optimal case at 130^o. They have been included to highlight the shape of the input pulse and the pulse train for different CEP. We can conclude that a good control over the CEP is needed to guarantee the optimal isolation of the attosecond pulse.

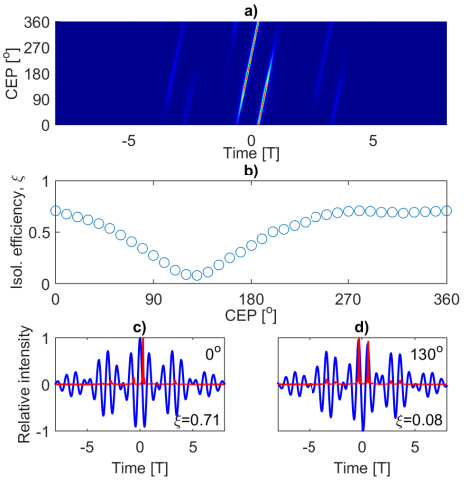

Fig. 5. Results obtained varying the CEP with a pulse of FWHM $\tau = 25$ fs and a frequency ratio of $\omega_2/\omega_1 = 1.3$. (a) A 2D map shows the temporal shape of the pulse train varying the CEP, the signal is normalized to the most intense pulse for each CEP. The isolation efficiency for each CEP is shown in (b). (c) and (d) show the input pulse (blue) and the corresponding attosecond pulse train (red), both normalized to the unity, at (c) $CEP = 0^o$ and (d) $CEP = 130^o$.

To summarize the results obtained from the parametric scan, Fig. 6 shows the optimal frequency ratio and the maximum isolation efficiency found for each FWHM. It depicts how as the pulse FWHM increases, the frequency ratio for an optimal result decreases and the isolation efficiency in the best scenario decreases as well, which establishes a limitation to isolate an attosecond pulse with a given FWHM. Interestingly, this decrease slows down as the FWHM increases, reaching a limit value for the frequency ratio of 1.2, while on the other hand the isolation efficiency decreases as the FWHM increases, as expected.

3. Effect of pre-plasmas

In all previous simulations it has been used a steep plasma profile, in which density grows from zero to the assumed solid density with a step-like function. In order to present a more realistic approach, since the plasmas in solid targets are generated by pre-pulses of the main laser pulse (much less intense and longer in time) or by the initial part of the laser pulse in the case of having

Optics EXPRESS

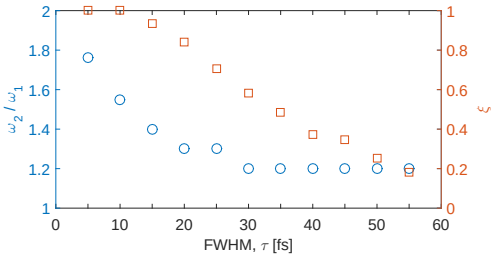

Fig. 6. Frequency ratio (blue circles) for the optimal isolation and the associated isolation efficiency (red squares) for each FWHM.

a good contrast, we analize the effect of the existence of a pre-plasma for the proposed gating technique. In the case of having a pre-pulse, the electrons and ions generated by ionization at the plasma surface will expand towards the vacuum before the main pulse arrives to the target, generating a front density region in which the density grows smoothly. The existence of such region strongly affects the laser-plasma interaction and its outcome, therefore unless a high contrast laser pulse is considered, the pre-plasma is expected to affect the obtained results.

To adress the effect of pre-plasmas, we have chosen the optimal frequency setup for three different pulse widths of 15, 20 and 25 fs, in this way we will be able to observe the effect of the pre-plasma and if it is dependent on the pulse width. We have analized how the isolation efficiency and the intensity of the most intense pulse change with the length of the pre-plasma region. Figure 7 displays the effect of the existence of a pre-plasma in the (a) isolation efficiency and (b) intensity of the most intense ultrashort pulse. We assume that the plasma density (n) grows exponentially in the pre-plasma region, from zero to the solid density (n_0) [8, 22, 30], with a function of the form: $n/n_0 = e^{log(2)(x-x_0+L)/L} - 1$, where $x \in [x_0 - L,\ x_0]$. The length L is defined as the scale length.

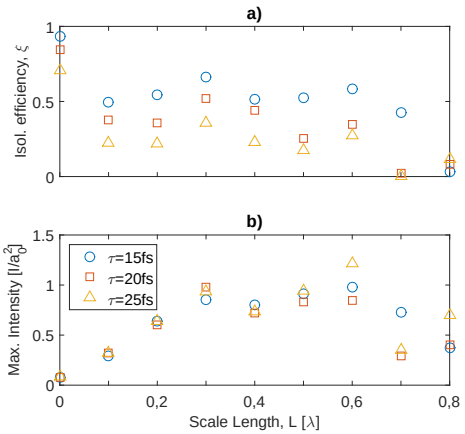

Fig. 7. Effect of the pre-plasma on the gating technique displayed in the (a) isolation efficiency and (b) intensity of the most intense pulse of the train. The frequency ratio is chosen as the optimal one for each FWHM, that is $\omega_2/\omega_1 = 1.4$ for $\tau = 15$ fs and $\omega_2/\omega_1 = 1.3$ for $\tau = \{20,\ 25\}$ fs.

Figure 7 depicts, for the three FWHM studied, that although the intensity of the central pulse grows substantially for a group of scale lengths, the isolation efficiency lowers as the scale length increases, which means that not only the most intense pulse is poorly isolated, but due

Optics EXPRESS

to its increase in intensity, the accompaning pulses will be also more intense in absolute terms. The isolation efficiency, in Fig. 7(a), experiences a decrease as soon as the pre-plasma is taken into account, and it keeps approximately constant until it drops to zero. The maximum intensity on the pulse train, in Fig. 7(b), experiences a similar trend, having a linear growth until an scale length of 0.3λ and a plateau for the rest of scale lengths, with a slight decrease for the highest scale lengths evaluated. Both plots show two local maxima at the scale lengths of 0.3λ and 0.6λ, respectively. This behaviour could be related to the fundamental processes of HHG in overdense targets, since long pre-plasma regions change the balance between the different absorption mechanisms and modify the particle dynamics at the plasma surface [7]. The growth of approximately one order of magnitude of the peak intensity in the attosecond pulse train is in agreement with previous results obtained by other authors, that show how the efficiency is lower when the density has a steep profile than when there is a pre-plasma [7, 8]. These results demonstrate that the existence of a pre-plasma region will be detrimental for the functioning of this gating technique.

4. Conclusions

It has been proven that the combination of two laser pulses of equal amplitude and envelope, with a properly tuned small frequency shift between them, creates a beating pattern that yields to the isolation of a single attosecond pulse once high harmonic orders have been filtered in the reflected field. This frequency gating works well for a wide range of FWHM below $\sim$ 35 fs, being able to isolate one or a few attosecond pulses. The experimental implementation of this method would require a good control over the central frequency of the two pulses involved and the carrier envelope phase, as it has been proven that it can affect the shape of the attosecond pulse train substantially. The existence of pre-plasmas has been proven detrimental for this gating techinque, therefore its optimal implementation would require the use of high contrast laser pulses. Its impact could be interesting in comparison with other gating methods, being an additional way to isolate attosecond pulses.

Funding

European Union and the Spanish Ministry of Economy and Competitivity (MINECO) (MAT2015-71119-R AEI/FEDER); Xunta de Galicia/FEDER (Agrup2015/11 (PC034)); Spanish Ministry of Education, Culture and Sports (MECD) (FPU14/00289).

Acknowledgments

The authors would like to acknowledge the OSIRIS Consortium, consisting of UCLA and IST (Lisbon, Portugal) for the use of OSIRIS, for providing access to the OSIRIS framework.